Supplement of The Cryosphere, 17, 3761–3783, 2023
https://doi.org/10.5194/tc-17-3761-2023-supplement

The Cryosphere Open Access EGU

Supplement of

The stability of present-day Antarctic grounding lines – Part 2: Onset of irreversible retreat of Amundsen Sea glaciers under current climate on centennial timescales cannot be excluded

Ronja Reese et al.

Correspondence to: Ronja Reese (ronja.reese@northumbria.ac.uk)

Table S1. Temperature corrections and melt rates for Antarctic basins with PICO parameters C =2.0 $\mathrm{Svm^3kg^{-1}}$ and $\gamma_T^\star$ =5.0 $\times 10^{-5}\mathrm{ms^{-1}}$.

basin	m_{obs} (Gt/yr)	δT (K)	m_{PICO} (Gt/yr)	m_{B_1} (m/yr)	m_{B_2} (m/yr)
1	75.2	0.17	74.18	1.27	-0.14
2	38.2	-0.03	38.72	2.68	0.44
3	17.1	-0.24	16.22	1.92	0.14
4	57.9	-0.15	55.32	2.63	0.55
5	6.8	-0.51	6.32	1.41	-0.13
6	29.3	-0.15	30.53	1.76	-1.46
7	79.2	0.07	76.71	6.75	2.57
8	89.3	-1.13	88.52	8.89	1.39
9	24.4	-0.39	25.74	3.78	0.66
10	7.6	-0.75	7.51	2.05	-1.45
11	7.4	-0.15	7.62	3.45	0.15
12	135.1	0.35	137.83	1.50	0.02
13	167.0	-1.10	164.69	6.88	2.63
14	236.4	-1.35	236.45	19.61	11.09
15	68.5	-2.00	222.18	13.15	6.63
16	143.1	-2.00	171.91	11.97	5.91
17	6.5	-1.23	6.46	18.36	17.62
18	67.8	-0.38	65.97	2.69	0.64
19	4.7	-0.15	4.39	1.19	-0.63

We use m_{obs} which are observational melt rates from Adusumilli et al. (2020). The temperature corrections δT are applied to the input temperature, and m_{PICO}, m_{B_1} and m_{B_2} denote melt rates calculated by PICO for the respective basin and boxes.

Table S2. Temperature corrections and melt rates for Antarctic basins with PICO parameters C =1.0 $\mathrm{Svm^3kg^{-1}}$ and $\gamma_T^\star$ =4.0 $\times 10^{-5}\mathrm{ms^{-1}}$.

basin	m_{obs} (Gt/yr)	δT (K)	m_{PICO} (Gt/yr)	m_{B_1} (m/yr)	m_{B_2} (m/yr)
1	75.2	0.52	76.35	1.09	-0.09
2	38.2	0.15	39.31	2.59	0.49
3	17.1	-0.09	16.48	1.83	0.17
4	57.9	0.02	57.98	2.63	0.58
5	6.8	-0.48	6.33	1.35	-0.03
6	29.3	0.02	28.02	1.42	-1.03
7	79.2	0.27	79.33	6.84	2.69
8	89.3	-0.93	88.41	8.47	1.96
9	24.4	-0.32	24.81	3.55	0.73
10	7.6	-0.72	7.30	1.80	-0.99
11	7.4	-0.11	6.92	2.97	0.26
12	135.1	0.75	132.34	1.38	0.04
13	167.0	-0.85	164.64	6.90	2.55
14	236.4	-0.93	234.56	19.59	10.96
15	68.5	-2.00	141.53	9.05	3.96
16	143.1	-1.70	144.18	10.63	4.79
17	6.5	-0.98	6.51	18.50	17.56
18	67.8	-0.16	66.52	2.66	0.69
19	4.7	-0.10	5.00	1.12	-0.44

We use m_{obs} which are observational melt rates from Adusumilli et al. (2020). The temperature corrections δT are applied to the input temperature, and m_{PICO}, m_{B_1} and m_{B_2} denote melt rates calculated by PICO for the respective basin and boxes.

Table S3. Temperature corrections and melt rates for Antarctic basins with PICO parameters C =3.0 $\mathrm{Svm^3kg^{-1}}$ and $\gamma_T^\star$ =4.0 $\times 10^{-5}\mathrm{ms^{-1}}$.

basin	m_{obs} (Gt/yr)	δT (K)	m_{PICO} (Gt/yr)	m_{B_1} (m/yr)	m_{B_2} (m/yr)
1	75.2	0.00	78.07	1.38	-0.10
2	38.2	-0.08	38.91	2.55	0.55
3	17.1	-0.29	16.27	1.84	0.24
4	57.9	-0.18	60.62	2.65	0.71
5	6.8	-0.51	5.68	1.26	-0.11
6	29.3	-0.25	30.08	1.74	-1.31
7	79.2	0.05	77.65	5.98	2.75
8	89.3	-1.10	91.12	8.56	2.27
9	24.4	-0.39	24.37	3.36	0.84
10	7.6	-0.75	7.58	1.92	-1.13
11	7.4	-0.15	7.21	3.05	0.28
12	135.1	0.12	131.34	1.43	0.05
13	167.0	-1.13	170.38	6.45	3.05
14	236.4	-1.30	236.22	18.19	11.79
15	68.5	-2.00	232.13	12.34	7.28
16	143.1	-2.00	201.46	11.86	7.07
17	6.5	-1.00	6.57	18.65	18.21
18	67.8	-0.43	70.12	2.73	0.81
19	4.7	-0.15	4.99	1.24	-0.58

We use m_{obs} which are observational melt rates from Adusumilli et al. (2020). The temperature corrections δT are applied to the input temperature, and m_{PICO}, m_{B_1} and m_{B_2} denote melt rates calculated by PICO for the respective basin and boxes.

Table S4. Temperature corrections and melt rates for Antarctic basins with PICO parameters C =3.0 $\mathrm{Svm^3kg^{-1}}$ and $\gamma_T^\star$ =7.0 $\times 10^{-5}\mathrm{ms^{-1}}$.

basin	m_{obs} (Gt/yr)	δT (K)	m_{PICO} (Gt/yr)	m_{B_1} (m/yr)	m_{B_2} (m/yr)
1	75.2	0.07	78.24	1.55	-0.23
2	38.2	-0.13	36.77	2.78	0.28
3	17.1	-0.31	15.90	2.06	0.04
4	57.9	-0.23	57.59	2.93	0.52
5	6.8	-0.53	6.27	1.47	-0.25
6	29.3	-0.23	31.20	2.12	-2.09
7	79.2	-0.03	80.04	7.62	2.54
8	89.3	-1.27	86.17	9.56	0.05
9	24.4	-0.46	24.31	3.96	0.22
10	7.6	-0.78	6.64	2.24	-2.25
11	7.4	-0.19	7.95	4.09	-0.18
12	135.1	0.17	132.64	1.54	-0.04
13	167.0	-1.25	163.64	7.21	2.46
14	236.4	-1.68	232.45	20.25	10.35
15	68.5	-2.00	320.98	18.77	9.65
16	143.1	-2.00	251.75	17.21	8.70
17	6.5	-1.48	6.56	18.64	17.87
18	67.8	-0.48	69.46	2.93	0.58
19	4.7	-0.16	4.99	1.50	-0.89

We use m_{obs} which are observational melt rates from Adusumilli et al. (2020). The temperature corrections δT are applied to the input temperature, and m_{PICO}, m_{B_1} and m_{B_2} denote melt rates calculated by PICO for the respective basin and boxes.

Table S5. Temperature corrections and melt rates for Antarctic basins with PICO parameters C =1.0 $\mathrm{Svm^3kg^{-1}}$ and $\gamma_T^\star$ =9.0 $\times 10^{-5}\mathrm{ms^{-1}}$.

basin	m_{obs} (Gt/yr)	δT (K)	m_{PICO} (Gt/yr)	m_{B_1} (m/yr)	m_{B_2} (m/yr)
1	75.2	0.92	76.70	1.27	-0.17
2	38.2	0.10	39.51	2.90	0.24
3	17.1	-0.09	16.72	2.09	-0.03
4	57.9	-0.03	58.83	3.05	0.40
5	6.8	-0.52	6.64	1.54	-0.25
6	29.3	0.15	28.58	1.73	-1.78
7	79.2	0.12	77.25	8.58	1.82
8	89.3	-1.13	88.14	10.23	-0.58
9	24.4	-0.41	25.36	4.42	-0.05
10	7.6	-0.75	6.94	2.30	-2.25
11	7.4	-0.17	7.26	4.09	-0.51
12	135.1	1.07	135.57	1.49	-0.02
13	167.0	-1.00	169.15	8.31	1.83
14	236.4	-1.40	237.50	23.80	8.70
15	68.5	-2.00	202.88	14.58	4.76
16	143.1	-1.85	144.60	13.27	3.86
17	6.5	-1.58	6.63	18.90	16.82
18	67.8	-0.21	69.12	2.88	0.55
19	4.7	-0.13	4.73	1.23	-0.66

We use m_{obs} which are observational melt rates from Adusumilli et al. (2020). The temperature corrections δT are applied to the input temperature, and m_{PICO}, m_{B_1} and m_{B_2} denote melt rates calculated by PICO for the respective basin and boxes.

Table S6. Summary of ensemble indicators. RMSE stands for root-mean-square deviation in ice thickness (h) or ice stream velocities (v) to present-day observations. We further test for deviations in grounded and floating area, and the average distance to the observed grounding line position. We calculate the average rate of ice thickness change. The last dimension is the difference to observed sea-level trend. We lay a specific focus on the Amundsen region (ASE), Filchner-Ronne (FRIS) and Ross (RIS) ice shelves by additionally evaluating each indicator for these drainage basins individually.

indicator	AIS1	AIS2	AIS3	AIS4	AIS5	AIS6	AIS7	AIS8	AIS9	AIS10	AIS11	AIS12	AIS13	AIS14	AIS15	AIS16	AIS17	AIS18	AIS19	AIS20	AIS21
RMSE(h)$_{AIS}$ (m)	335.65	344.50	349.50	347.75	348.02	347.63	345.03	344.92	348.71	345.37	341.46	343.40	345.89	344.49	343.37	342.85	341.65	340.92	343.83	343.65	342.37
RMSE(h)$_{ASE}$ (m)	172.62	182.90	192.72	182.70	191.34	187.77	173.75	185.03	194.93	185.39	167.93	193.79	184.16	191.74	184.16	199.80	185.60	203.30	201.87	197.09	221.61
RMSE(h)$_{RIS}$ (m)	268.56	276.04	286.65	281.10	275.89	286.01	268.20	268.99	271.40	265.43	264.46	267.27	263.32	263.58	256.77	262.12	257.55	257.86	261.68	257.62	256.24
RMSE(h)$_{FRIS}$ (m)	240.53	247.34	256.51	242.43	249.94	253.41	241.91	240.85	256.63	248.36	226.36	242.13	236.00	236.04	235.60	244.13	228.03	238.00	228.89	225.56	228.62
RMSE(v)$_{AIS}$ (m/a)	257.61	250.28	247.51	263.44	250.92	252.23	276.08	249.11	244.55	253.32	297.70	260.78	275.21	272.92	272.29	247.34	305.83	255.27	275.49	306.04	299.63
RMSE(v)$_{ASE}$ (m/a)	74.84	68.47	69.46	67.66	68.52	65.51	80.71	72.32	68.32	75.41	100.74	72.72	94.67	87.11	85.68	77.92	122.60	95.78	98.00	127.17	147.09
RMSE(v)$_{RIS}$ (m/a)	33.39	31.86	33.32	33.28	34.56	32.97	36.33	32.64	34.83	33.71	36.67	40.23	33.01	34.82	38.26	37.18	36.40	34.47	35.92	37.22	35.13
RMSE(v)$_{FRIS}$ (m/a)	24.19	23.49	22.60	23.34	22.83	22.46	23.67	23.35	22.82	24.33	25.19	23.91	23.58	23.69	25.19	23.67	24.78	24.57	24.39	24.67	25.36
ΔA^g_{AIS} (km^2)	685440	693504	706880	695040	718016	707136	690368	713088	729664	722368	671296	726336	709376	721152	713600	731648	680128	727872	710464	698752	712704
ΔA^g_{ASE} (km^2)	8512	8192	7104	7936	8128	7808	8704	9088	8256	9152	10112	10496	10112	11072	10432	11648	12800	15232	14976	15168	19072
ΔA^g_{RIS} (km^2)	128256	123904	125312	127552	134656	128256	125376	140096	135744	137728	132160	153024	144128	153856	143552	151360	130240	154368	155520	145856	155776
ΔA^g_{FRIS} (km^2)	109056	114496	119808	106816	113664	116864	111744	106240	119616	116992	97664	105216	102400	102016	107136	109312	102016	106688	96256	98176	99648
ΔA^f_{AIS} (km^2)	567296	578816	592192	576064	588544	587904	577600	582400	601280	592000	558592	600768	580928	598976	584896	605312	568384	602688	585472	570048	587584
ΔA^f_{ASE} (km^2)	8896	9792	9472	9408	13312	9664	10048	11200	13184	11264	11008	14976	12800	16704	12800	16320	13440	18176	17472	15552	21440
ΔA^f_{RIS} (km^2)	85760	81152	82432	84992	92288	85632	82880	97856	93248	95360	89664	111040	101888	112192	101184	109248	87680	112192	113920	103680	113728
ΔA^f_{FRIS} (km^2)	97344	102656	107776	94976	101824	105088	99584	94272	107776	105216	85760	93376	90432	90368	94976	97536	89984	95104	84416	86336	87744
ΔGL_{AIS} (km)	9.47	9.78	9.76	10.24	10.27	10.03	9.82	10.56	10.54	10.27	9.82	11.18	10.66	11.20	10.70	11.13	10.14	11.43	11.05	10.59	11.16
ΔGL_{ASE} (km)	6.67	7.05	6.83	6.47	6.02	6.43	6.70	6.90	6.03	7.09	8.56	8.21	8.45	9.56	8.23	9.66	11.16	14.67	13.80	13.00	18.01
ΔGL_{RIS} (km)	21.40	19.76	19.91	21.22	23.89	21.00	20.20	25.64	24.23	24.73	23.15	29.63	27.65	30.56	26.69	29.41	22.93	30.54	31.26	28.34	31.32
ΔGL_{FRIS} (km)	12.47	13.63	13.36	14.91	13.84	13.55	13.22	15.01	14.38	12.49	12.92	14.93	14.23	13.95	14.50	14.74	13.96	14.32	13.12	13.01	13.67
dhdt$_{AIS}$ (mm/a)	83.70	86.64	83.01	86.30	69.36	81.55	87.13	71.76	69.35	72.12	91.51	62.82	76.11	64.79	79.10	62.28	96.45	63.76	64.64	80.96	71.86
dhdt$_{ASE}$ (mm/a)	95.57	99.81	93.98	91.59	71.98	105.42	97.27	76.76	67.36	89.45	124.36	77.03	101.71	89.79	102.01	86.84	143.86	70.09	82.65	125.65	139.86
dhdt$_{RIS}$ (mm/a)	43.14	42.35	40.16	44.47	34.15	40.46	44.35	35.98	37.26	34.72	45.03	30.73	35.26	28.63	37.82	29.95	44.92	29.80	31.75	37.92	31.38
dhdt$_{FRIS}$ (mm/a)	39.16	37.64	39.82	40.65	33.84	39.04	38.91	35.34	32.98	32.42	39.17	27.59	34.90	26.97	34.38	27.35	39.62	27.14	27.35	34.24	28.36
ΔSLE (mm)	6.25	5.71	6.22	6.17	8.10	6.73	5.96	7.39	7.96	8.13	5.16	8.88	7.45	7.50	6.47	9.00	2.79	7.65	8.57	5.67	6.93

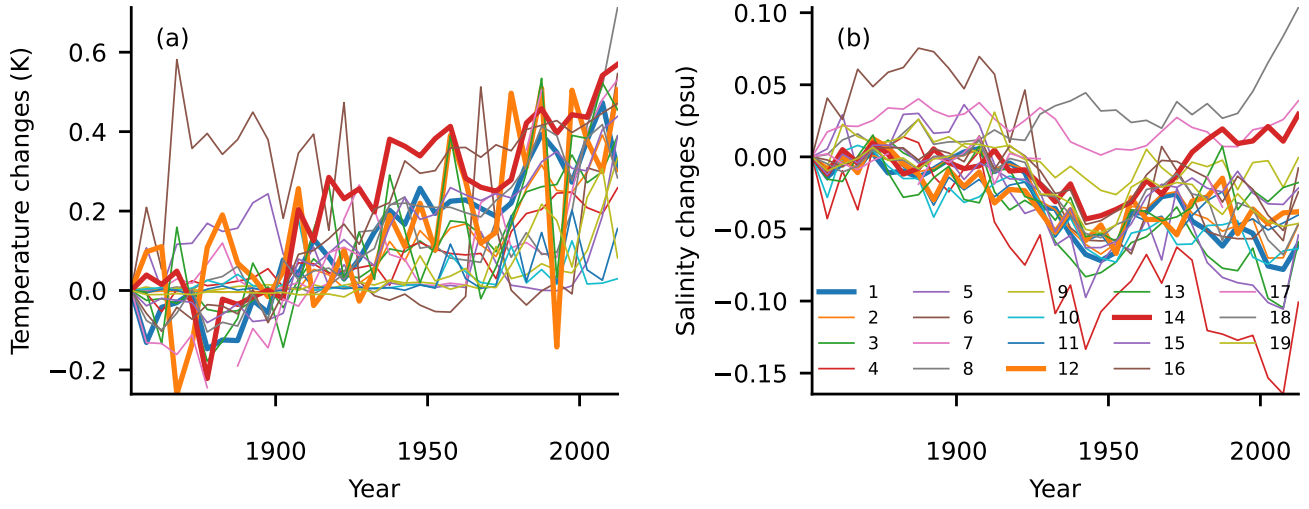

Figure S1. Historic increase in (a) ocean temperatures and (b) salinities as input into PICO box 0. Basin 1 corresponds to Filchner-Ronne Ice Shelf, basin 12 to Ross Ice Shelf and basin 14 covers the Amundsen Sea. All basins are as in Reese et al. (2018).

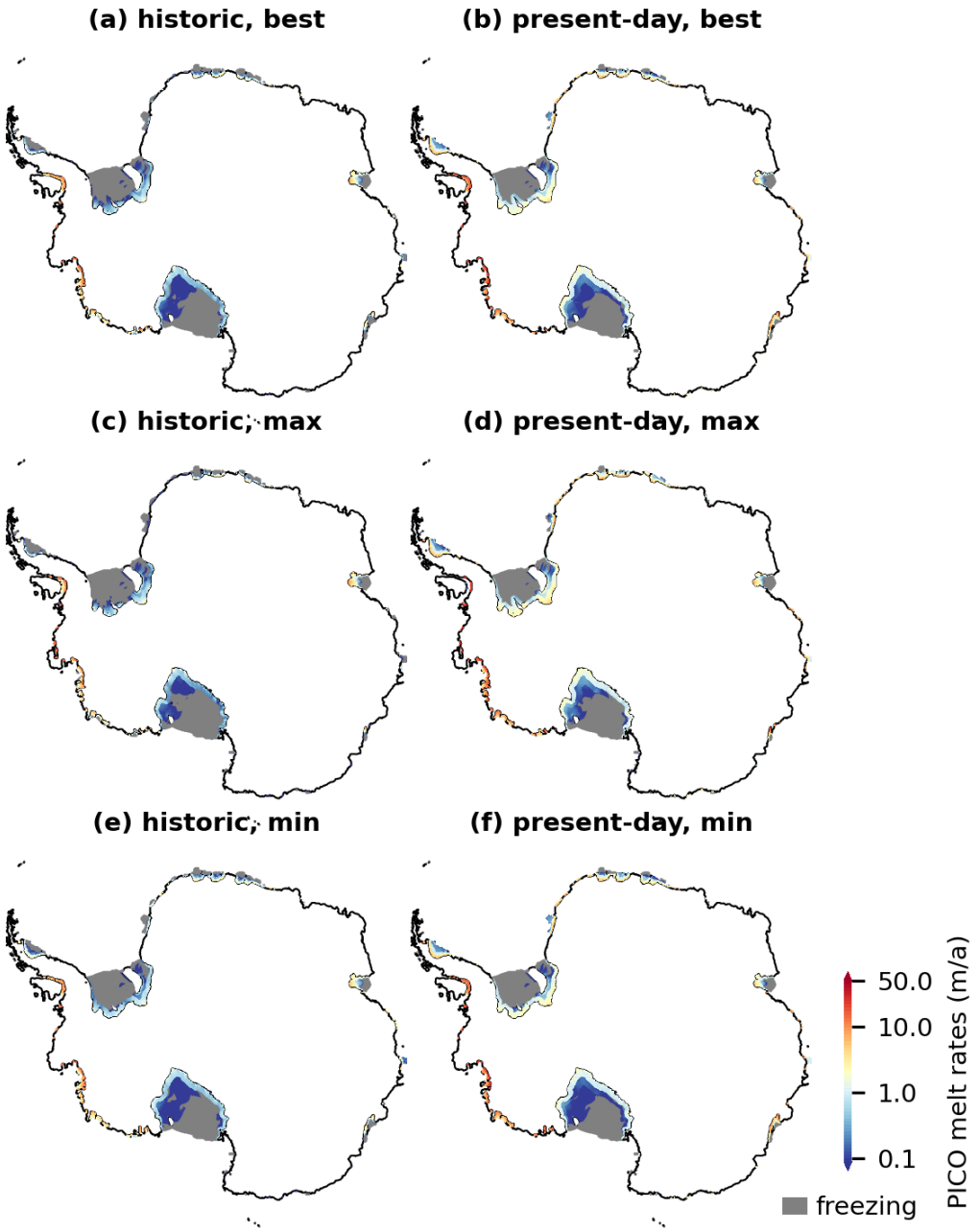

Figure S2. PICO basal melt rates for the 'best' PICO parameters for the AIS5 configuration in (a) the historic control run, and (b) the present-day extended run, the 'max' PICO parameters in the AIS1 configuration in (c) the historic control run, and (d) the present-day extended run, and the 'min' PICO parameters in the AIS12 configuration in (e) the historic control run, and (f) the present-day extended run.

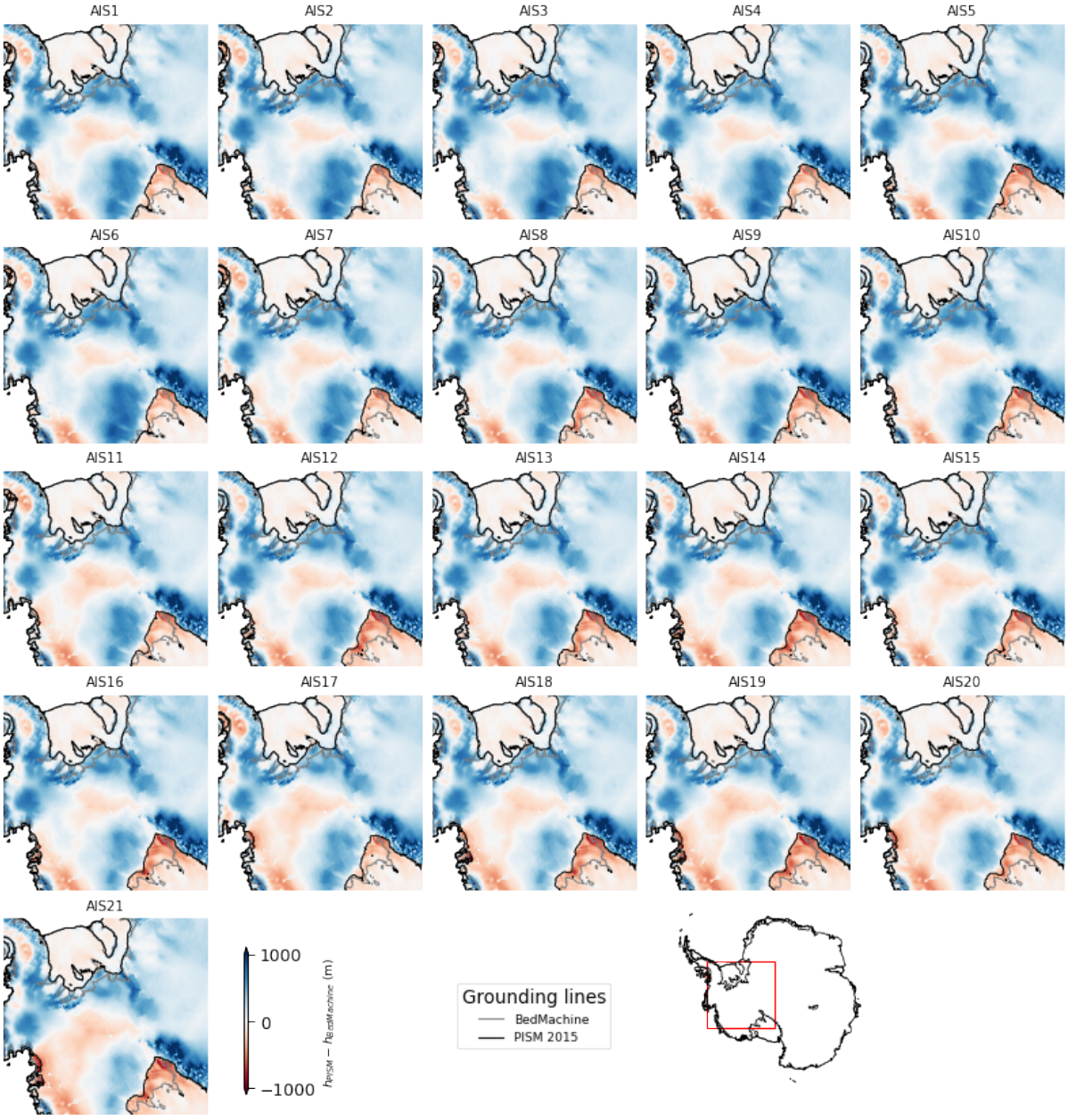

Figure S3. Grounding lines and ice thickness changes relative to BedMachine in ensemble members in 2015, zoomed into the West Antarctic Ice Sheet. Inset shows zoom location.

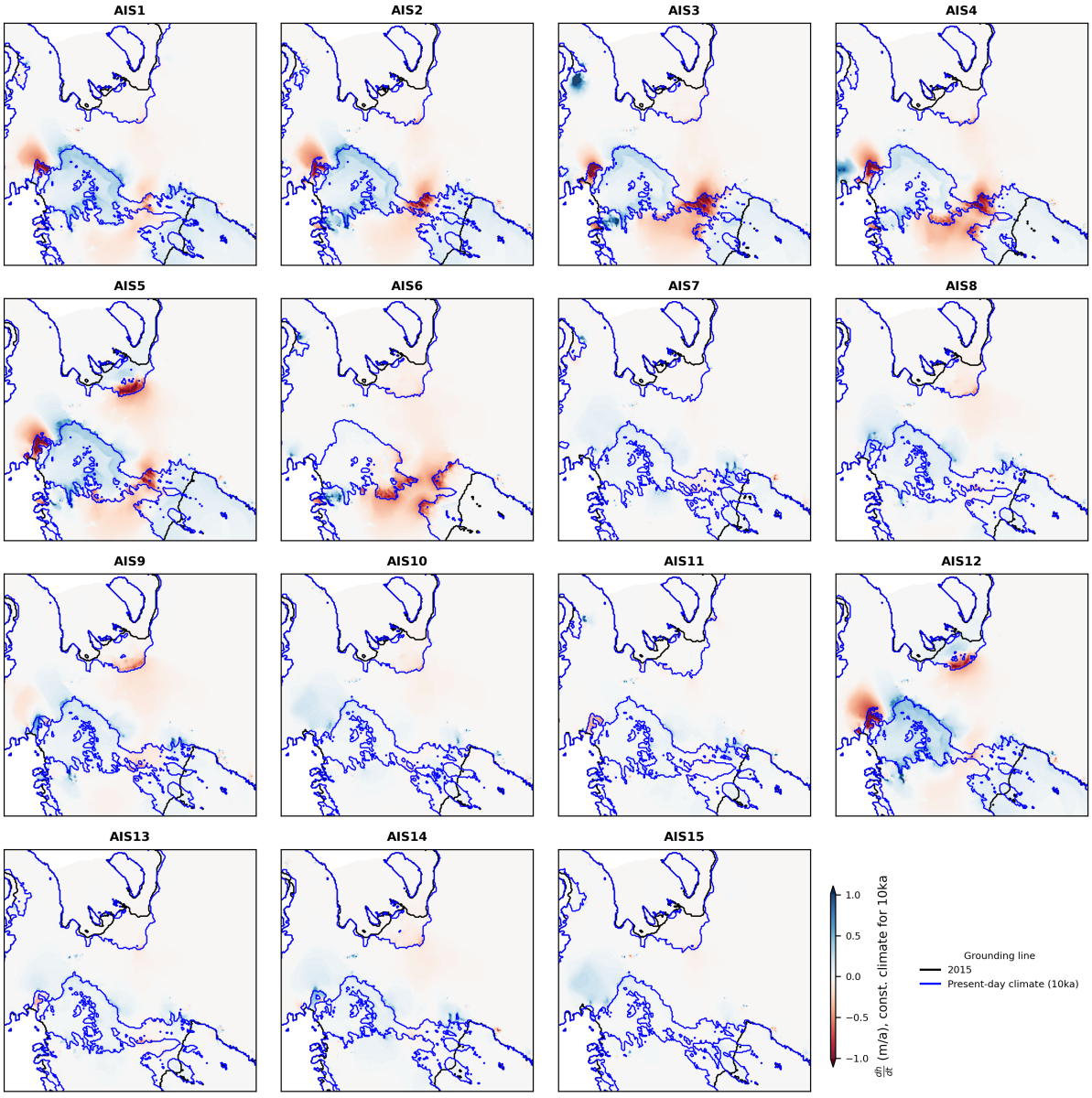

Figure S4. Long-term evolution for all AIS configurations, zoomed into the West Antarctic Ice Sheet (same region as in Fig. S3). The 2015 grounding line positions are shown in black. Over 10,000 years of constant present-day climate the grounding lines evolve to the positions shown in blue. The spatial map shows the rates of ice thickness changes after 10,000 years of constant present-day climate forcing.

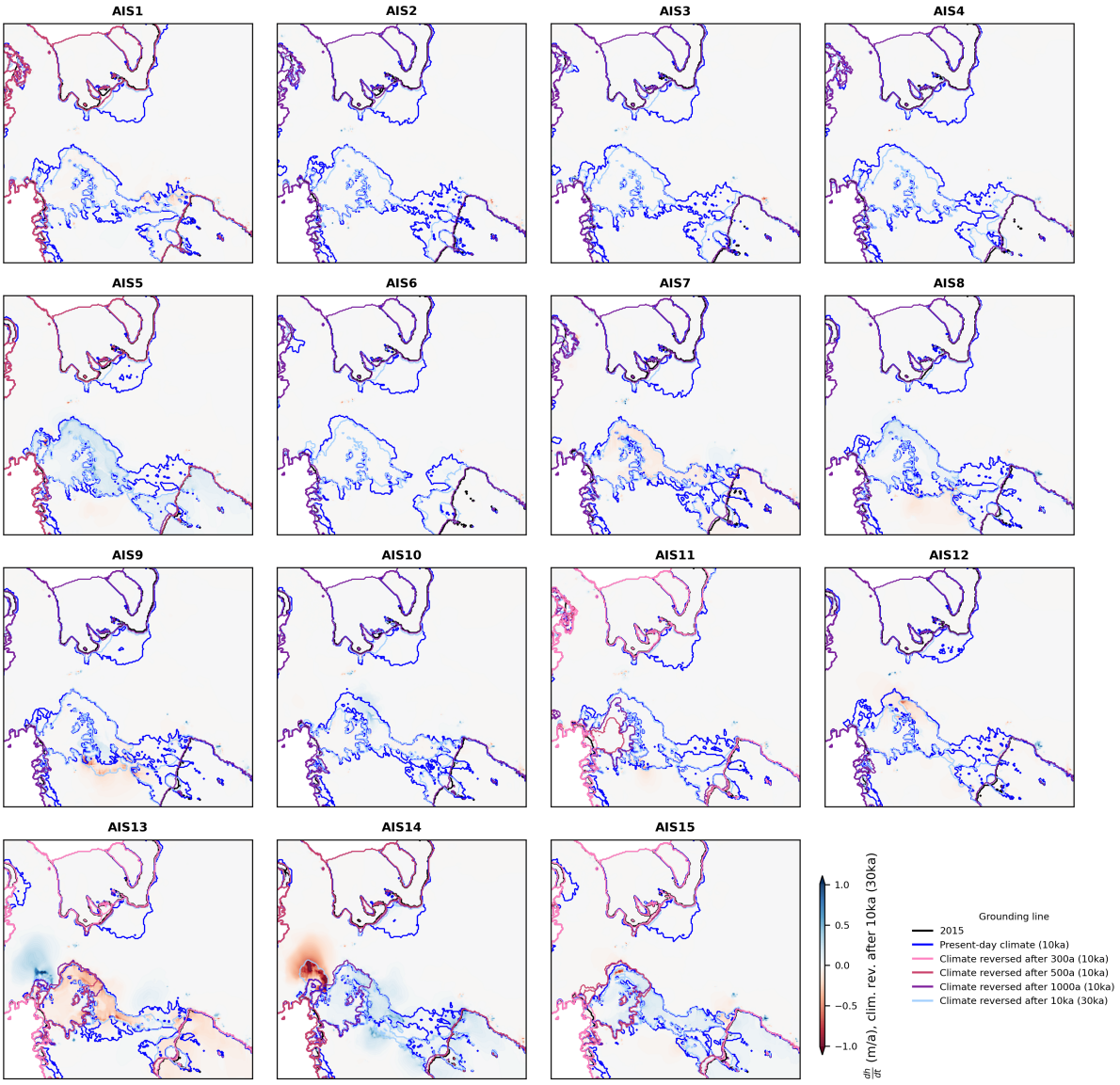

Figure S5. Long-term evolution and reversibility for all AIS configurations, zoomed into the West Antarctic Ice Sheet (same region as in Fig. S3). The 2015 grounding line positions are shown in black. Over 10,000 years of constant present-day climate the grounding lines evolve to the positions shown in blue. When reversing the climate to historic conditions after 300, 500 or 1000 years, they evolve to the positions shown in pink, dark pink and purple, respectively. When reversing the climate to historic conditions after 10,000 years and continuing the runs for another 20,000 years, the grounding lines evolve to the positions shown in light blue. The spatial map shows the rates of ice thickness changes after 20,000 years of reversed forcing.

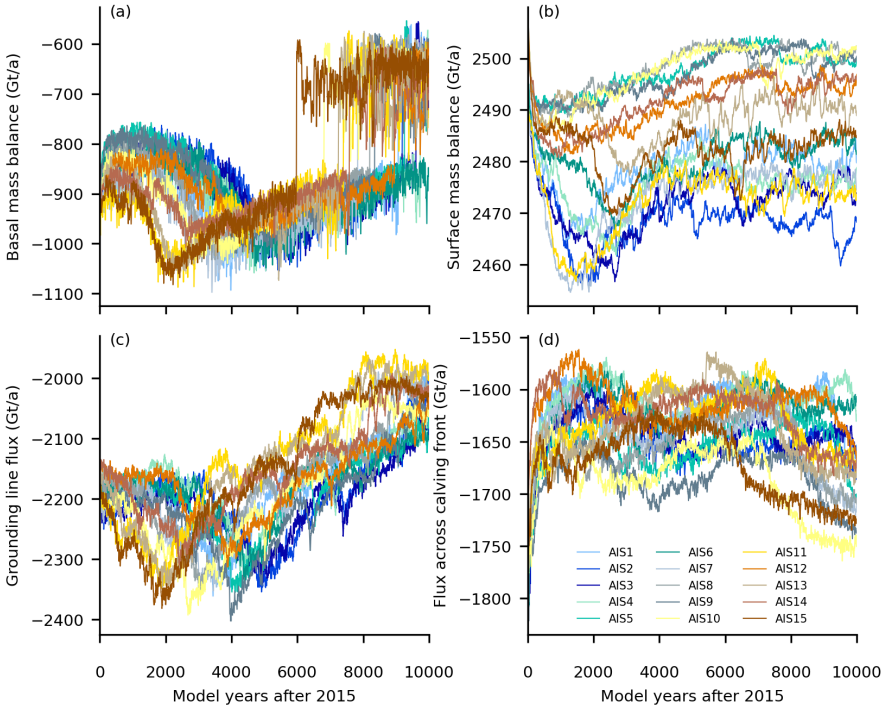

Figure S6. Evolution of the basal mass balance (only over floating regions), the surface mass balance, the grounding line flux and the flux across the calving front which is kept at its present-day location for all ensemble members over the 10,000 years of constant present-day climate conditions. Values are 25-year running means.

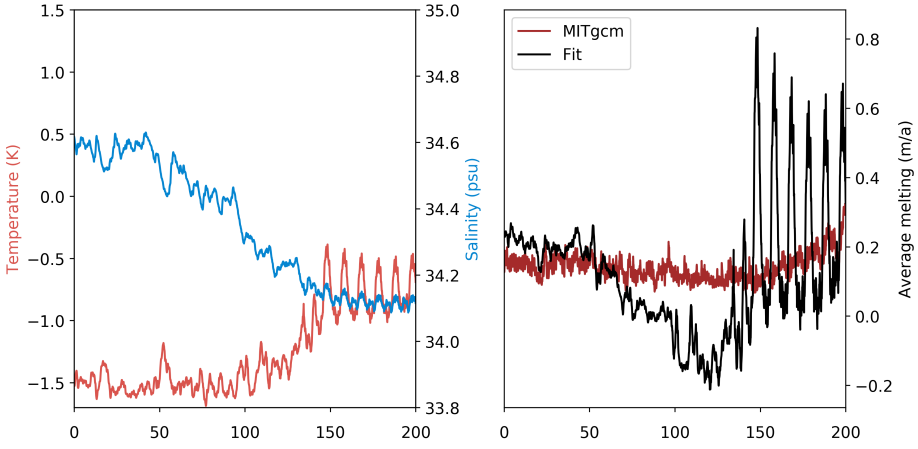

Figure S7. Testing the Filchner-Ronne Ice Shelf melt relationship for a different ocean simulation. Left panel: evolution of average ocean temperature and salinity at the depth of the continental shelf in front of the ice shelf in the ocean simulations of the Weddell Sea in Naughten et al. (2021) for the 1 percent CO2 increase scenario. Right panel: modelled and predicted melt rates using the fitted function from Appendix A1.

References

Adusumilli, S., Fricker, H. A., Medley, B., Padman, L., and Siegfried, M. R.: Interannual variations in meltwater input to the Southern Ocean from Antarctic ice shelves, Nature Geoscience, 13, 616–620, https://doi.org/10.1038/s41561-020-0616-z, 2020.

Naughten, K. A., Rydt, J. D., Rosier, S. H. R., Jenkins, A., Holland, P. R., and Ridley, J. K.: Two-timescale response of a large Antarctic ice shelf to climate change, Nature Communications, 12, https://doi.org/10.1038/s41467-021-22259-0, 2021.

Reese, R., Albrecht, T., Mengel, M., Asay-Davis, X., and Winkelmann, R.: Antarctic sub-shelf melt rates via PICO, The Cryosphere, 12, 1969–1985, https://doi.org/10.5194/tc-12-1969-2018, 2018.